



# Journal of Applied and Computational Mechanics



Research Paper

## Dynamic Response of a Step Loaded Cubic Cavity Embedded in a Partially Saturated Poroelastic Half-space by the Boundary Element Method

Andrey Petrov<sup>1</sup>, Mikhail Grigoryev<sup>1</sup>, Leonid Igumnov<sup>1</sup>, Aleksandr Belov<sup>1</sup>, Victor Eremeyev<sup>2,3</sup>

<sup>1</sup> National Research Lobachevsky State University of Nizhny Novgorod, 23 Gagarin av. bld. 6, Nizhny Novgorod, 603950, Russia

<sup>2</sup> Department of Mechanics of Materials and Structures, Faculty of Civil and Environmental Engineering, Gdansk University of Technology, 11/12 Gabriela Narutowicza Street, Gdansk, 80-233, Poland

<sup>3</sup> Department of Civil and Environmental Engineering and Architecture (DICAAR), University of Cagliari, Via Marengo, 2, 09123 Cagliari, Italy

Received September 07 2021; Revised November 05 2021; Accepted for publication November 16 2021.

Corresponding author: A. Petrov (andrey.petrov@mech.unn.ru)

© 2022 Published by Shahid Chamran University of Ahvaz

**Abstract.** The boundary element method is used to analyze the problem of dynamic loading acting inside a cubic cavity located in a partially saturated poroelastic halfspace. Defining relations of a Biot's porous medium are used, which are written in Laplace representations for unknown functions of displacements of the skeleton and pore pressures of the fillers. Solutions in time are obtained using the stepped method of numerical inversion of Laplace transforms. Dynamic responses of displacements and pore pressures at points on the surface of the halfspace and the cavity have been constructed. The effect of the values of the saturation coefficient and of the depth of the location of the cavity on dynamic responses has been studied.

**Keywords:** Poroelastic half-space, embedded cubic cavity, step load, boundary element method, Laplace transform.

### 1. Introduction

Processes determined by a dynamic effect from various perturbation sources on solid bodies containing cavities and inclusions represent a class of topical problems of modern mechanics, which have a wide scope of application and are highly important in engineering practice. For instance, in geomechanics and mining, when analyzing the stress-strain state of rocks near mining workings, the geometry of the mined-out space can be approximated by a spherical cavity. When analyzing such problems, the theory of deformation of rock masses or soils as a heterogeneous medium is normally used, their dynamics being described by the well-developed linear theory of propagation of elastic and viscoelastic waves. However, in a number of cases, a poroelastic medium model must be used that makes it possible to describe the filtration of the filler in the pores, in combination with a full-scale mechanical model of the stress-strain state of the medium. Even with considerable simplifications, using a model of such a liquid-saturated porous material substantially complicates the computational scheme of the boundary-value problem, as compared with elastic or viscoelastic formulations, and calls for developing adequate mathematical and methodological tools and related software. Use of the boundary element method (BEM) in analyzing the class of problems in question is justified by its key advantages: its numerical-analytical nature, the relatively random geometry of boundary surfaces, automatic provision of the conditions of behavior over infinity in semi-infinite bodies. Scientific literature abounds in studies on modeling the dynamics of poroelastic bodies and media containing cavities and inclusions, in which analytical [1-5], semi-analytical [6-8] and numerical [9-13] methods are applied. However, the results published in them pertain only to either two-dimensional problems [14] or to wave scattering problems [15], or were obtained using the model of a fully saturated poroelastic material. Fundamental solutions of the three-dimensional dynamic theory of partially saturated poroelastic media, required for implementing the boundary-element methodology, are presented in [16], but without the results of the analysis of the problem. Based on somewhat different dynamic equations of poroelastic media, [17] also derives fundamental solutions and analyzes problems of wave propagation as a result of a load acting on a half-space surface. Results of boundary-element modeling of wave processes in partially saturated poroelastic bodies are also given in [18, 19]. The present paper uses the boundary element method to analyze the problem of dynamic loading acting inside a cubic cavity located in a partially saturated poroelastic half-space. The effect of the value of the saturation coefficient and of the depth of the location of the cavity on dynamic responses is studied.



## 2. Governing Equations

The mathematical model of the problem will be written following the approach of Schanz and Li [17]. A poroelastic medium is represented using the following mathematical model of a heterogeneous material: an elastic skeleton phase (s) and two filler phases – a liquid (w) and a gas (a) filling the pore system. The sealed pores are considered as part of the solid. All the three phases are assumed to be compressible. Temperature variations are neglected. Such a poroelastic material can be considered as partially saturated, and its model is called a three-phase model. The relative proportions of constituent volumes are characterized by its porosity  $\varphi$  and saturation degrees  $S_f$  as

$$\varphi = \frac{V_v}{V}, \quad S_f = \frac{V_f}{V}, \quad (f = w; a), \quad (1)$$

where  $V_v$  is volume of interconnected pores in the specimen,  $V$  is total volume of the material,  $V_f$  is volume of the filler. This gives the average density of the mixture  $\rho$  as:

$$\rho = \rho_s(1 - \varphi) + \varphi S_w \rho_w + \varphi S_a \rho_a, \quad (2)$$

where  $\rho_s$ ,  $\rho_w$  and  $\rho_a$  are partial densities of each phase. Consider a case where the pores are completely filled:

$$S_a + S_w = 1. \quad (3)$$

The following equation suggested by Bishop [20] for the effective stress in partially saturated porous media is used assuming the Bishop's parameter is identical to the saturation degree  $S_w$  and also incorporating the Biot's effective stress  $\alpha$ :

$$\sigma_{ij} = \sigma_{ij}^{eff} - \delta_{ij} \alpha (S_w p^w + S_a p^a), \quad (4)$$

where  $\sigma_{ij}^{eff}$  is the effective stress,  $\sigma_{ij}$  represents the total stress,  $p^w$  is the pore water pressure,  $p^a$  denotes the pore air pressure and  $\delta_{ij}$  is the Kronecker delta. The Biot's coefficient  $\alpha$  is described by the relationship:

$$\alpha = 1 - \frac{K}{K_s}, \quad (5)$$

where  $K$  is the bulk modulus of the porous media and  $K_s$  is the bulk modulus of the solid grains. The relation between stress and strain in the solid skeleton under assumption of its isotropic linear elastic behavior is given by:

$$\sigma_{ij}^{eff} = 2G \varepsilon_{ij}^s + \left( K - \frac{2}{3} G \right) \varepsilon_{kk}^s, \quad (6)$$

where  $G$  is the shear modulus. Assuming the small strain gradients the kinematic relation is given in the following form:

$$\varepsilon_{ij}^s = \frac{1}{2} (u_{i,j}^s + u_{j,i}^s), \quad (7)$$

where  $u_i^s$  is the solid displacements. To construct equations of motion, constitutive equations must be combined with the related balance equations of momentum and balance equations of mass of each of the phases [17]. The linear momentum balance equation for each fluid phase results in the generalized Darcy equation for multiphase flow as:

$$\varphi S_w q_i^f = -k_f (p_{,i}^f + \rho_j \dot{u}_i^s + \rho_j \dot{q}_i^f), \quad (f = w; a), \quad (8)$$

where  $q_i^f$  represents the Darcy velocity and  $k_f$  is the phase permeability. The phase permeability  $k_f$  is defined as:

$$k_f = \frac{K_{rf} k}{\eta_f}, \quad (9)$$

where  $k$  is the intrinsic permeability matrix of the poroelastic material,  $K_{rf}$  is the relative phase permeability,  $\eta_f$  is the viscosity of the filler. The relative permeability of the liquid phase  $K_{rw}$  and the gas phase  $K_{ra}$  are obtained from:

$$K_{rw} = S_e^{(2+3\theta)/\theta}, \quad K_{ra} = (1 - S_e)^2 [1 - S_e^{(2+\theta)/\theta}], \quad (10)$$

in which  $\theta$  is the pore size distribution index and  $S_e$  is the effective liquid saturation given by

$$S_e = \frac{S_w - S_{rw}}{S_{ra} - S_{rw}}, \quad (11)$$

where  $S_{rw}$  is the residual liquid-saturation,  $S_{ra}$  is the residual gas-saturation.

In a partially saturated porous material containing two non-mixing fillers the interface surface between them is curved as a result of intermolecular interaction forces. The accompanying pressure difference in both of the interfacing phases is called capillary pressure  $p^c$ . Capillary pressure can be represented as a function of the saturation degree as follows:

$$p^c = p^a - p^w = p^d S_e^{-1/\theta}, \quad (12)$$

where  $p^d$  is the gas pressure required for driving the liquid out of the pores.



Using a Laplace transform assuming vanishing initial conditions makes it possible to write down a precise form of the governing equations in Laplace transform domain in terms of spatial derivatives of solid displacements  $u_i^s$  as well as liquid and gas pressures  $p^w$  and  $p^a$ . The final differential equations in the Laplace domain are arranged into matrix product form as follows:

$$\begin{bmatrix} B_1 \delta_{ij} + B_2 \partial_i \partial_j & B_3 \partial_i & B_4 \partial_i \\ B_5 \partial_j & B_6 & B_7 \\ B_8 \partial_j & B_9 & B_{10} \end{bmatrix} \begin{bmatrix} \hat{u}_i \\ \hat{p}^w \\ \hat{p}^a \end{bmatrix} = \begin{bmatrix} -\hat{F}_i \\ -\hat{I}^w \\ -\hat{I}^a \end{bmatrix}, \quad \mathbf{x} \in \Omega, \quad \Omega \subset \mathbf{R}^3 \tag{13}$$

where

$$B_1 = G\nabla^2 - (\rho - \beta S_w \rho_w - \gamma S_a \rho_a) s^2, \quad B_2 = K + \frac{G}{3}, \quad B_3 = -(\alpha - \beta) S_w, \tag{14}$$

$$B_4 = -(\alpha - \gamma) S_a, \quad B_5 = -(\alpha - \beta) S_w s, \quad B_6 = -\left( \zeta S_{ww} S_w + \frac{\varphi}{K_w} S_w - S_u \varphi \right) s + \frac{\beta S_w}{\rho_w s} \nabla^2, \tag{15}$$

$$B_7 = -(\zeta S_{aa} S_w + S_u \varphi) s, \quad B_8 = -(\alpha - \gamma) S_a s, \quad B_9 = -(\zeta S_{ww} S_a + S_u \varphi) s, \tag{16}$$

$$B_{10} = -\left( \zeta S_{aa} S_a + \frac{\varphi}{K_a} S_a - S_u \varphi \right) s + \frac{\gamma S_a}{\rho_a s} \nabla^2, \quad S_u = -\frac{\theta(S_{ra} - S_{rw})}{p^d} S_e^{(\theta+1)/\theta}, \tag{17}$$

$$\zeta = \frac{\alpha - \varphi}{K_s}, \quad \beta = \frac{\kappa_w \varphi \rho_w s}{\varphi S_w + \kappa_w \rho_w s}, \quad \gamma = \frac{\kappa_a \varphi \rho_a s}{\varphi S_a + \kappa_a \rho_a s}, \tag{18}$$

$$S_{ww} = S_w - \theta(S_w - S_{rw}), \quad S_{aa} = S_a + \theta(S_w - S_{rw}). \tag{19}$$

In the Eq. (13)  $\hat{F}_i$  denotes bulk body force per unit volume,  $\hat{I}^w$  and  $\hat{I}^a$  denote fluid source terms, and hat symbol denotes Laplace transform with complex variable  $s$ .

A generalized displacement vector and a generalized force vector are additionally introduced as

$$\mathbf{u}(\mathbf{x}, s) = (\hat{u}_1^s, \hat{u}_2^s, \hat{u}_3^s, \hat{p}^w, \hat{p}^a), \tag{20}$$

$$\mathbf{t}(\mathbf{x}, s) = (\hat{t}_1^s, \hat{t}_2^s, \hat{t}_3^s, -\hat{q}^w, -\hat{q}^a), \tag{21}$$

where  $\hat{t}_i^s = \hat{\sigma}_{ij}^{eff} n_j$  and  $\hat{q}^f = \hat{q}_i^f n_i$ ,  $n_i$  are components of the vector of the normal to the boundary of region  $\Omega$ .

Equation (13), supplemented with boundary conditions:

$$\mathbf{u}(\mathbf{x}, s) = \bar{\mathbf{u}}, \quad \mathbf{x} \in \Gamma^u, \tag{22}$$

$$\mathbf{t}(\mathbf{x}, s) = \bar{\mathbf{t}}, \quad \mathbf{x} \in \Gamma^\sigma, \tag{23}$$

where  $\Gamma^u$  is the Dirichlet's boundary and  $\Gamma^\sigma$  is the Neumann's boundary, fully describe the boundary problem in the representations of the 3D isotropic dynamic theory of poroelasticity.

### 3. Boundary Element Method Framework

Boundary-value problem (13), (22), (23) is solved using the direct boundary element method, based on a combined use of integral Laplace transform and boundary integral equation (BIE) of the 3D isotropic theory of poroelasticity:

$$\mathbf{C}(\mathbf{y}) \mathbf{u}(\mathbf{y}, s) + \int_{\Gamma} \mathbf{T}(\mathbf{x}, \mathbf{y}, s) \mathbf{u}(\mathbf{y}, s) d\Gamma = \int_{\Gamma} \mathbf{U}(\mathbf{x}, \mathbf{y}, s) \mathbf{t}(\mathbf{y}, s) d\Gamma, \quad \mathbf{x}, \mathbf{y} \in \Gamma, \tag{24}$$

where  $\mathbf{U}(\mathbf{x}, \mathbf{y}, s)$  and  $\mathbf{T}(\mathbf{x}, \mathbf{y}, s)$  are matrices of fundamental and singular solutions, respectively,  $\mathbf{x}$  is an integration point,  $\mathbf{y}$  is an observation point. The values of the coefficients of matrix  $\mathbf{C}$  are defined by the geometry of boundary  $\Gamma$ . A procedure for obtaining BIE's, based on the weighted residual method can be found in [21]. Some of the problems of the arising kernels of BIE's are discussed in [22].

Equations (24) comprise singular integrals in the sense of Cauchy, which are quite difficult to compute. Use of the boundary properties of retarded potentials makes it possible, based on [23], to write down a regular representation of equation (18):

$$\int_{\Gamma} (\mathbf{T}(\mathbf{x}, \mathbf{y}, s) \mathbf{u}(\mathbf{x}, s) - \mathbf{T}^0(\mathbf{x}, \mathbf{y}, s) \mathbf{u}(\mathbf{y}, s) - \mathbf{U}(\mathbf{x}, \mathbf{y}, s) \mathbf{t}(\mathbf{x}, s)) d\Gamma = 0, \quad \mathbf{x}, \mathbf{y} \in \Gamma, \tag{25}$$

where  $\mathbf{T}^0(\mathbf{x}, \mathbf{y}, s)$  is singularity matrix. Using Equation (25), it is possible to construct a boundary-element solution of the BIE.



In the result of spatial discretization, boundary  $\Gamma$  is represented with a set of  $K_E$  quadrangular eight-node boundary elements. The geometry of each element  $E_k$  is defined by biquadratic functions of form  $N_m$  and the global coordinates of nodes  $\mathbf{x}_m^k$ , related as [24]

$$\mathbf{x}(\xi) = \sum_{m=1}^8 N_m(\xi) \mathbf{x}_m^k, k = 1 \dots K, \quad (26)$$

where  $\xi = (\xi_1, \xi_2) \in (-1, 1)^2$  are local coordinates. According to correlated interpolation model [25], displacements are described using bilinear elements with the related bilinear functions of form  $R_l(\xi)$ , and surface generalized forces are described with constant boundary elements:

$$\mathbf{u}(\xi) = \sum_{l=1}^4 R_l(\xi) \mathbf{u}_l^k, \quad (27)$$

$$\mathbf{t}(\xi) = \mathbf{t}^k, \quad (28)$$

where  $\mathbf{u}_m^k$  and  $\mathbf{t}^k$  are nodal values of displacements and tractions, respectively, over element  $E_k$ .

A discrete representation of BIE's written at the nodes of the approximation of boundary functions  $\mathbf{y}^i$ , using the collocation method and accounting for (26)-(28), is of the following form:

$$\sum_{k=1}^{K_E} \sum_{m=1}^4 \Delta \mathbf{T}_{mi}^k \mathbf{u}_m^k = \sum_{k=1}^{K_E} \Delta \mathbf{U}_i^k \mathbf{t}^k, \quad (29)$$

$$\Delta \mathbf{U}_i^k = \int_{-1}^1 \mathbf{U}(\mathbf{x}^k(\xi), \mathbf{y}^i, s) J^k(\xi) d\xi, \quad (30)$$

$$\Delta \mathbf{T}_{mi}^k = \int_{-1}^1 [R_m(\xi) \mathbf{T}(\mathbf{x}^k(\xi), \mathbf{y}^i, s) - \mathbf{I} \cdot \mathbf{T}^0(\mathbf{x}^k(\xi), \mathbf{y}^i)] J^k(\xi) d\xi, \quad (31)$$

where  $\mathbf{I}$  is unit matrix,  $J^k$  is Jacobian of the local coordinates into global ones.

The elements of matrices  $\Delta \mathbf{U}_i^k$ ,  $\Delta \mathbf{T}_{mi}^k$  are computed using numerical integration schemes depending on the kind of integral (nonsingular or singular). Nonsingular integrals arise, when the collocation point does not belong to the element. Here, standard Gaussian-type formula is used in combination with a hierarchical subdivision of the elements [26]. Singular integrals arise, when the collocation point is situated on the element being integrated over. In this case, new local coordinates are introduced, making it possible to avoid a singularity in the integrand and to use Gaussian integration.

#### 4. Laplace Transform Inversion

Consider a method based on the fundamental integration theorem – the stepped method of numerical inversion of Laplace transform. Consider the following integral:

$$y(t) = \int_0^t f(\tau) d\tau, \quad (32)$$

Integral (32) gives rise to Cauchy problem for an ordinary differential equation:

$$\frac{d}{dt} x(t) = s x(t, s) + C, \quad x(0) = 0. \quad (33)$$

Integral (32) is substituted for by a quadrature sum, weighting factors of which are determined using Laplace representation and the linear multistep method [27]. Further derivation is based on the results of this work. The traditional stepped method of integrating the original is that integral (32) is calculated using the following relation:

$$y(0) = 0, \quad y(n\Delta t) = \sum_{k=1}^n \omega_k(\Delta t), \quad n = 1, \dots, N, \quad (34)$$

$$\omega_n(\Delta t) = \frac{R^{-n}}{L} \sum_{l=0}^{L-1} \hat{f} \left( \frac{\gamma(R e^{2il\pi/L})}{\Delta t} \right) e^{-2inl\pi/L}, \quad (35)$$

where  $\Delta t$  is time step,  $\gamma(z) = 3/2 - 2z + z^2/2$ ,  $N$  is number of time steps,  $R$  is the parameter of the method.

#### 5. Numerical Results and Analysis

Using the above methodology and the related software realized on its basis, a problem of a load acting inside a cubic cavity of edge  $2m$  embedded in a partially saturated poroelastic half-space is analyzed (Fig. 1). A load applied to the cavity surface linearly increases up to time  $0.01s$  and then acquires a constant value of  $10000N/m^2$ .



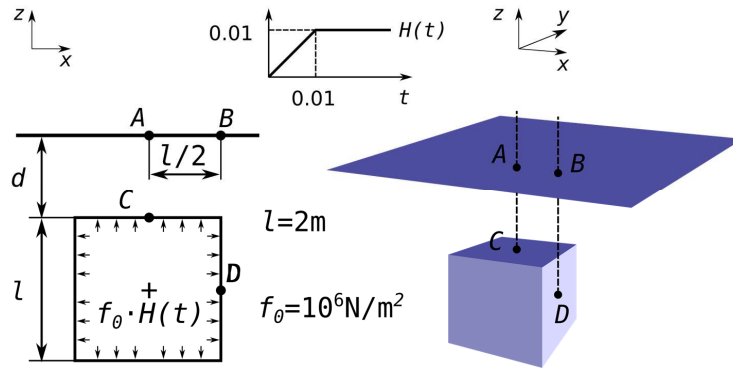


Fig. 1. Geometry of the problem.

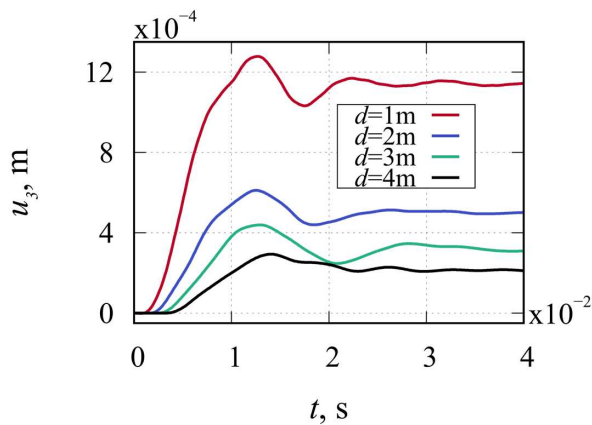


Fig. 2. Effect of  $d$  on  $u_3$  at point A.

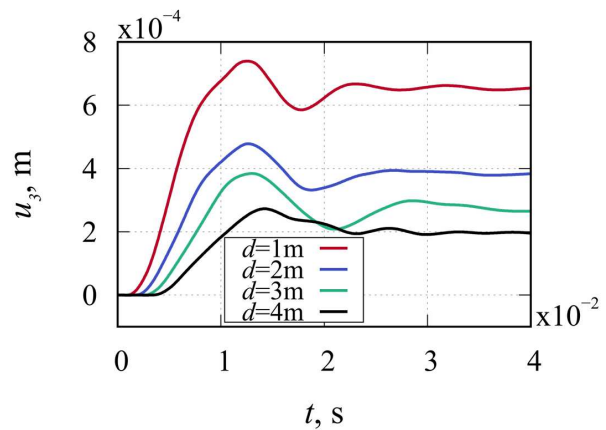


Fig. 3. Effect of  $d$  on  $u_3$  at point B.

Zero boundary conditions for filler flows are also assigned over the cavity surface. The half-space surface is permeable and load-free. The material parameters of the poroelastic half-space are summarized in Table 1. Time history of unknown functions is examined for the following parameters of the stepped method:  $R = 0.997$ ,  $N = 500$ ,  $\Delta t = 0.00008s$ . Dynamic responses of the displacements and pore pressures at the points on the half-space surface situated directly above the cavity and at the center points of the cavity sides are constructed.

The effect of the depth of the cavity on dynamic response has been analyzed for four different values of parameter  $d$ :  $1m$ ,  $2m$ ,  $3m$ ,  $4m$ . The saturation degree of the material is taken to be  $0.9$ . The results of the corresponding numerical analyses are presented in Figs. 2-7.

Table 1. General material parameters.

Parameter type	Symbol	Value	Unit
Porosity	$\varphi$	0.23	-
Density of the solid skeleton	$\rho_s$	2650	kg/m <sup>3</sup>
Density of the water	$\rho_w$	997	kg/m <sup>3</sup>
Density of the air	$\rho_a$	1.1	kg/m <sup>3</sup>
Drained bulk modulus of the mixture	$K$	$1.02 \cdot 10^9$	N/m <sup>2</sup>
Shear modulus of the mixture	$G$	$1.44 \cdot 10^9$	N/m <sup>2</sup>
Bulk modulus of the solid grains	$K_s$	$3.5 \cdot 10^{10}$	N/m <sup>2</sup>
Bulk modulus of the water	$K_w$	$2.25 \cdot 10^9$	N/m <sup>2</sup>
Bulk modulus of the air	$K_a$	$1.1 \cdot 10^5$	N/m <sup>2</sup>
Intrinsic permeability	$k$	$2.5 \cdot 10^{-12}$	m <sup>2</sup>
Viscosity of the water	$\eta_w$	$1.0 \cdot 10^{-3}$	N · s/m <sup>2</sup>
Viscosity of the air	$\eta_a$	$1.8 \cdot 10^{-5}$	N · s/m <sup>2</sup>
Gas entry pressure	$p^d$	$5 \cdot 10^4$	N/m <sup>2</sup>
Residual water saturation	$S_{rw}$	0	-
Residual air saturation	$S_{ra}$	1	-
Pore size distribution index	$\theta$	1.5	-



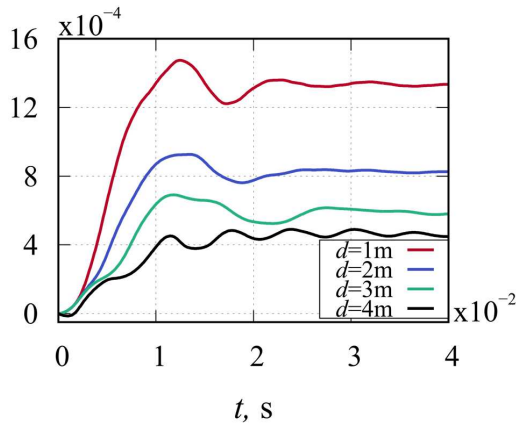


Fig. 4. Effect of  $d$  on  $u_3$  at point C.

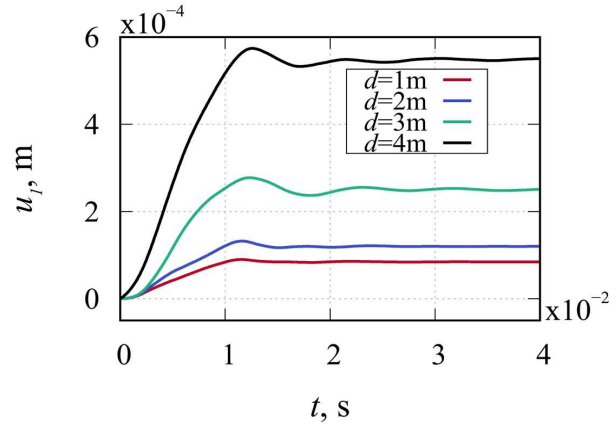


Fig. 5. Effect of  $d$  on  $u_1$  at point D.

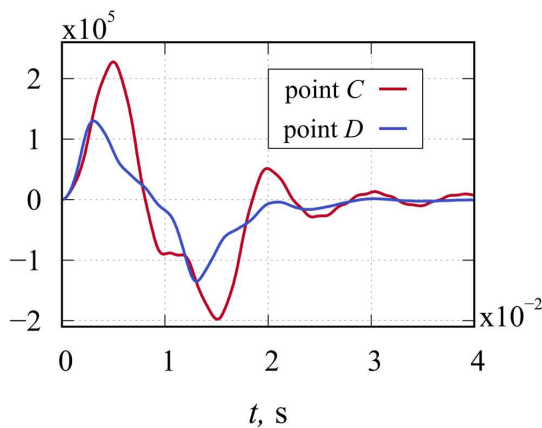


Fig. 6. Time history of  $p^w$  at points C and D for  $d = 4m$ .

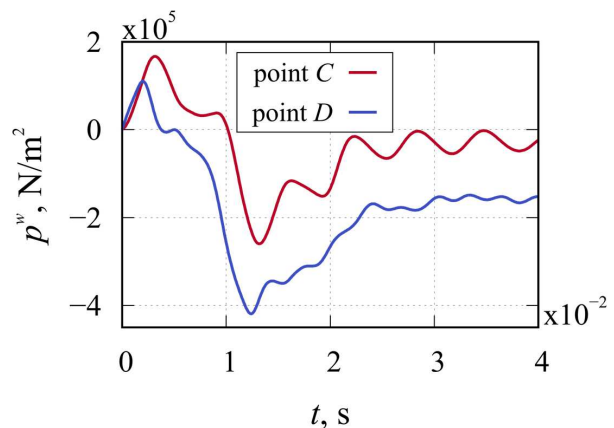


Fig. 7. Time history of  $p^w$  at points C and D for  $d = 1m$ .

It can be seen in Figs. 2-5 that the displacements at points A, B, C, D increase with the load and after a minor decrease become constant. At the same time, at points A, B, and C at a smaller depth, the displacements increase faster and acquire higher values than at bigger depths. Besides, the vertical displacements at point C are higher than those at points A and B for all values of  $d$ . At point D, an opposite trend is observed: at smaller depths, the horizontal displacements reach higher values faster than at smaller depths, and for  $d = 4m$  become close in their values to the vertical displacements at point C at the same depth.

Figures 6 and 7 show the dynamic responses of the pore pressure of the liquid at points C and D for  $d = 1m$  and  $d = 4m$ . In both cases, the pore pressure demonstrates similar behavior in time with differences in the values. For  $d = 1m$ , at points C and D, it increases up to the value of  $1.2 \cdot 10^5 N/m^2$  almost at the same rate, after which, it decreases at point D but continues to increase up to  $2.4 \cdot 10^5 N/m^2$  at point C. Having reached its maximum, the pressures at both points drop down to zero almost at the same time, then acquire negative values, return again to the zero value and remain at this level the rest of the time. For  $d = 4m$ , the pressures at points C and D, as in the first case, increase up to their maximal values almost at the same rate and then drop down to zero. However, the alteration of the pressure at point D occurs almost twice as fast as at point C. At the same time, the pressure at point D acquires a lower negative value than at point C, and, on the time interval considered, does not reach the constant zero value. Besides, the pressure amplitude for  $d = 4m$  is higher than that for  $d = 1m$  in both points.

The effect of the saturation degree on the dynamic response has been analyzed for four different values of parameter  $S_w = 0.5; 0.9; 0.95$ , as well as the limiting value 1 corresponding to full saturation of the material. The cavity is assumed to be situated at the depth of  $2m$ . The results of the corresponding numerical analyses are presented in Figs. 8-13.

It can be seen in Figs. 8-11 that, for all the considered values of  $S_w$ , the displacements at points A, B, C, D behave in the same way as was described earlier. However, for the values of  $S_w$  equal to 0.5, 0.9 and 0.95, the displacement curves are closer to one another and graphically are practically indiscernible. In the limiting case, the displacements increase more slowly and acquire smaller values than in the case of a partially saturated material.

The effect of the saturation degree shows itself to its maximum on the dynamic response of pore pressure (Fig. 12 and Fig. 13). It is seen that, for  $S_w = 0.9; 0.95$ , pressure behaves in the way described earlier. For  $S_w = 0.5$ , pressure grows more slowly and with a smaller amplitude as compared with the other cases, and acquires only positive values on the considered time interval. In the limiting case, pressure grows faster and with a larger amplitude than in the other cases, and acquires only positive values. At the same time, the pressure at point C has a larger amplitude than that at point D, as in the case with  $S_w = 0.9$  and  $d = 2m$ .



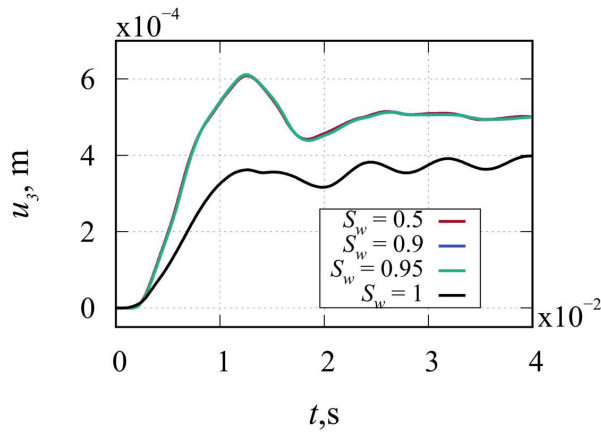


Fig. 8. Effect of  $S_w$  on  $u_3$  at point A.

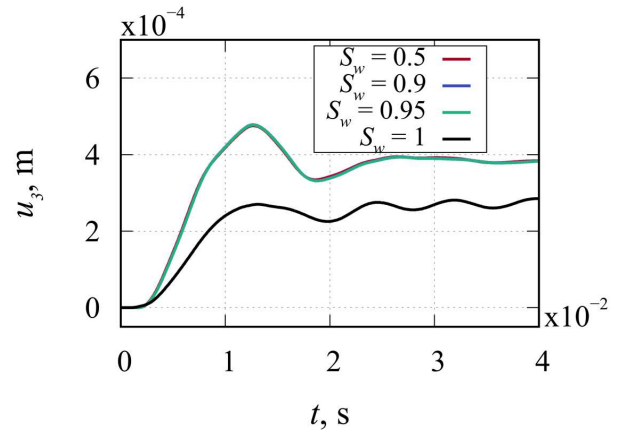


Fig. 9. Effect of  $S_w$  on  $u_3$  at point B.

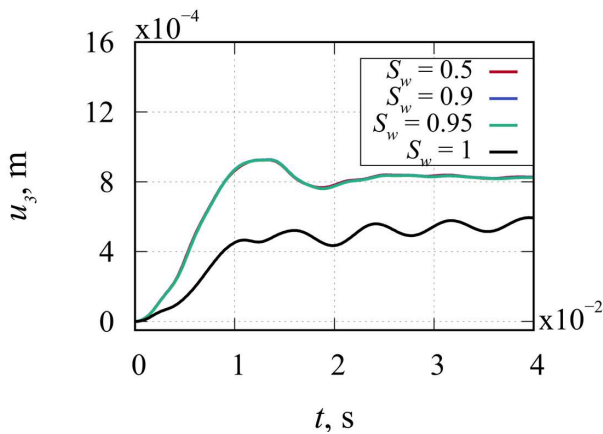


Fig. 10. Effect of  $S_w$  on  $u_3$  at point C.

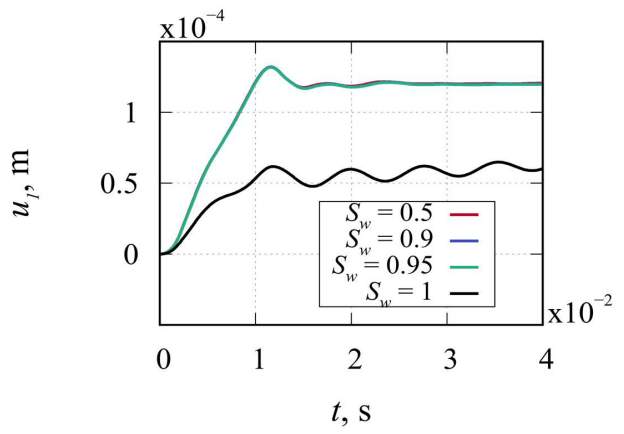


Fig. 11. Effect of  $S_w$  on  $u_1$  at point D.

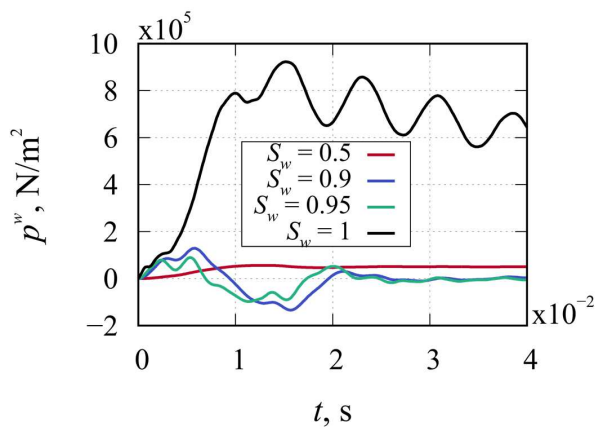


Fig. 12. Effect of  $S_w$  on  $p^w$  at point C.

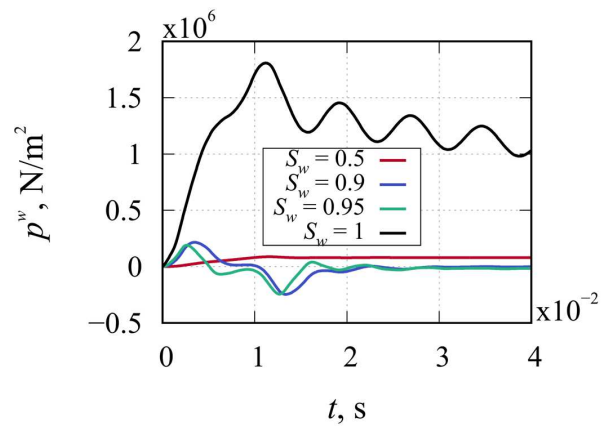


Fig. 13. Effect of  $S_w$  on  $p^w$  at point D.

### 6. Conclusion

The boundary-element approach and the apparatus of Laplace transform have been used in the numerical parametric study of the analysis of the problem of a dynamic load acting inside a cubic cavity situated in a partially saturated poroelastic half-space. The effect of the values of saturation degree and the depth of the position of the cavity on dynamic responses of displacements and pore pressures at points on the half-space and cavity surfaces has been analyzed. Based on the numerical analyses, the following conclusions have been drawn:

- At the points on the half-space surface and on the upper surface of the cavity, vertical displacements grow faster and acquire higher values as depth decreases. At the depth of 4m, the vertical displacements at both points on the half-space surface acquire close values, whereas the vertical displacement at the point on the surface of the upper side of the cavity acquires a value close to the horizontal displacement at the point on the side surface. That is, for values over 4m, the effect of depth on the dynamic response of displacements on the cavity surface is less pronounced.
- The increase of depth results in the increase of the horizontal displacement amplitude at the point on the side surface of the cavity but has almost no effect on the character of the behavior and amplitude of the vertical displacement at the point on the upper surface, which may be due to the relative proximity of the permeable interface of the half-space.
- The increase in the saturation degree from 0.5 to 0.95 practically does not affect the dynamic response of displacements



but shows to its maximum on the pore pressure response.

- Use of the model of a fully saturated material in this problem results in underestimating displacements and overestimating pore pressures.

To get a deeper insight into the related effects, comprehensive studies with various types of dynamic loading and geometries are required.

### Author Contributions

Basic idea of the paper was conceived by Leonid Igumnov. Victor Eremeev implemented these ideas and suggested the numerical experiments. Andrey Petrov conducted the literature survey and examined the BEM solution relevance. Aleksandr Belov performed the stability analysis and developed the FORTRAN codes. Aleksandr Belov and Andrey Petrov conducted the numerical experiments and examined the validity of results. Mikhail Grigoryev obtained the results in figures and tables. The manuscript was written through the contribution of all authors. All authors discussed the results, reviewed and approved the final version of the manuscript.

### Acknowledgement

Not applicable.

### Conflict of Interest

The authors declared no potential conflicts of interest concerning the research, authorship, and publication of this article.

### Funding

The theoretical study was done with financial support from the Ministry of Science and Higher Education of the Russian Federation (Project 0729-2020-0054). The numerical experiments were conducted with financial support from RFBR (Project 19-38-90224).

### Data Availability Statements

The datasets generated and/or analyzed during the current study are available from the corresponding author on reasonable request.

### References

- [1] Wang, Y., Gao, G.-Y., and Yang, J., Three-dimensional dynamic response of a lined tunnel in a half-space of saturated soil under internal explosive loading, *Soil Dynamics and Earthquake Engineering*, 101, 2017, 157–161.
- [2] Wen, M.-J., Xu, J.-M., Analytical solution for torsional vibration of a pile in saturated soil considering imperfect contact, *Gongcheng Lixue*, 31(7), 2014, 156–161.
- [3] Ozyazicioglu, M., Spherical wave propagation in a poroelastic medium with infinite permeability: Time domain solution, *The Scientific World Journal*, 2014, 2014, 1–10.
- [4] Schanz, M., Poroelastodynamics: Linear models, analytical solutions, and numerical methods, *Applied Mechanics Reviews*, 62(3), 2009, 1–15.
- [5] Karinski, Y.-S., Shershnev, V.-V., Yankelevsky, D.-Z., Analytical solution of the harmonic waves diffraction by a cylindrical lined cavity in poroelastic saturated medium, *International Journal for Numerical and Analytical Methods in Geomechanics*, 31(5), 2007, 667–689.
- [6] Wang, Y., Gao, G.-Y., Lin, J., Gao, M., Dynamic response of cylindrical lining in poroelastic saturated half-space soil induced by internal loading, 6th *International Symposium on Environmental Vibration*, Shanghai, China, 2013.
- [7] Gao, M., Gao, G., Wang, Y., The transient response of cylindrical lining in poroelastic saturated half-space, *Guti Lixue Xuebao*, 33(2), 2012, 219–226.
- [8] Zhou, X.-L., Wang, J.-H., Jiang, L.-F., Dynamic response of a pair of elliptic tunnels embedded in a poroelastic medium, *Journal of Sound and Vibration*, 325(4–5), 2009, 816–834.
- [9] Akhlaghi, T., Nikkar, A., Effect of vertically propagating shear waves on seismic behavior of circular tunnels, *The Scientific World Journal*, 2014, 2014.
- [10] Gao, M., Gao, G.-Y., Li, D.-Y., Transient response of lining structure subjected to sudden internal uniform loading considering effects of coupling mass, *Yantu Gongcheng Xuebao*, 33(6), 2011, 862–868.
- [11] Amorosi, A., Boldini, D., Numerical modelling of the transverse dynamic behaviour of circular tunnels in clayey soils, *Soil Dynamics and Earthquake Engineering*, 29(6), 2009, 1059–1072.
- [12] Rajapakse, R.-K.-N.-D., Senjuntichai, T., An indirect boundary integral equation method for poroelasticity, *International Journal for Numerical and Analytical Methods in Geomechanics*, 19(9), 1995, 587–614.
- [13] Kattis, S.-E., Beskos, D.-E., Cheng, A.-H.-D., 2D dynamic response of unlined and lined tunnels in poroelastic soil to harmonic body waves, *Earthquake Engineering and Structural Dynamics*, 32(1), 2003, 97–110.
- [14] He, C., Zhou, S., Di, H., Xiao, J., A 2.5-D coupled FE-BE model for the dynamic interaction between tunnel and saturated soil, *Lixue Xuebao*, 49(1), 2017, 126–136.
- [15] Yuan, Z., Boström, A., Cai, Y., Cao, Z., Closed-form analytical solution for vibrations from a tunnel embedded in a saturated poroelastic half space, *Journal of Engineering Mechanics*, 143(9), 2017, 04017079.
- [16] Ashayeri, I., Kamalian, M., Jafari, M.K., Gatzmiri, B., Analytical 3D transient elastodynamic fundamental solution of unsaturated soils, *International Journal for Numerical and Analytical Methods in Geomechanics*, 35(17), 2011, 1801–1829.
- [17] Li, P., and Schanz, M., Time domain boundary element formulation for partially saturated poroelasticity, *Engineering Analysis with Boundary Elements*, 37(11), 2013, 1483–1498.
- [18] Igumnov, L.A., Petrov, A.N., Belov, A.A., Mironov, A.A., Lyubimov, A.K., Dianov, D.Yu., Numerically-analytically studying fundamental solutions of 3-D dynamics of partially saturated poroelastic bodies, *Materials Physics and Mechanics*, 42(5), 2019, 596–601.
- [19] Igumnov, L.A., Petrov, A.N., Vorobtsov, I.V., The time-step boundary-element scheme on the nodes of the Lobatto method in problems of 3-D dynamic poroelasticity, *Materials Physics and Mechanics*, 42(1), 2019, 103–111.
- [20] Bishop, A. W., The principle of effective stress, *Teknisk Ukeblad*, 106(39), 1959, 859–863.
- [21] Schanz, M., *Wave Propagation in Viscoelastic and Poroelastic Continua: A Boundary Element Approach*, Springer-Verlag, Berlin Heidelberg, 2001.
- [22] Amenitsky, A.V., Belov, A.A., Igumnov, L.A., Karelin I.S., Granichnye integral'nye uravneniya dlya resheniya dinamicheskikh zadach trekhmernoj teorii porouprugosti (Boundary Integral Equations for Analyzing Dynamic Problems of 3-d Poroelasticity (in Russian)), *Problems of Strength and Plasticity*, 71, 2009, 164–171.
- [23] Igumnov, L.A., Litvinchuk, S.Yu., Petrov, A.N., Ipatov A.A., Numerically Analytical Modeling the Dynamics of a Prismatic Body of Two- and Three-Component Materials, *Advanced Materials*, 175, 2016, 505–516.
- [24] Bazhenov, V.G., Igumnov, L.A., *Metody granichnykh integral'nykh uravnenij i granichnykh elementov v reshenii zadach trekhmernoj dinamicheskoy teorii uprugosti s sopryazhennymi polyami (Boundary Integral Equations and Boundary Element Methods in Treating the Problems of 3D Elastodynamics with Coupled*






Fields (in Russian), PhysMathLit, Moscow, 2008.


[25] Goldshteyn, R.V., *Metod granichnyh integral'nyh uravnenij – sovremennyy vychislitel'nyj metod prikladnoj mekhaniki (Boundary Integral Equations Method: Numerical Aspects and Application in Mechanics)* (in Russian), Mir, Moscow, 1978.


[26] Lachat, J.C., Watson, J.O., Effective numerical treatment of boundary integral equations: A formulation for three-dimensional elastostatics, *International Journal for Numerical Methods in Engineering*, 10(5), 1976, 991–1005.


[27] Igumnov, L.A., Petrov, A.N., Modelirovanie dinamiki chastichno nasyschennyh porouprugih tel na osnove metoda granichno-vremennyh elementov (Dynamics of partially saturated poroelastic solids by boundary-element method) (in Russian), *PNRPU Mechanics Bulletin*, 3, 2016, 47–61.


## ORCID iD

Andrey Petrov  <https://orcid.org/0000-0001-5277-9384>

Mikhail Grigoryev  <https://orcid.org/0000-0002-4203-1775>

Leonid Igumnov  <https://orcid.org/0000-0003-3035-0119>

Aleksandr Belov  <https://orcid.org/0000-0003-3704-048X>

Victor Eremeyev  <https://orcid.org/0000-0002-8128-3262>



© 2022 Shahid Chamran University of Ahvaz, Ahvaz, Iran. This article is an open access article distributed under the terms and conditions of the Creative Commons Attribution-NonCommercial 4.0 International (CC BY-NC 4.0 license) (<http://creativecommons.org/licenses/by-nc/4.0/>).

**How to cite this article:** Petrov A., Grigoryev M., Igumnov L., Belov A., Eremeyev V. Dynamic Response of a Step Loaded Cubic Cavity Embedded in a Partially Saturated Poroelastic Half-space by the Boundary Element Method, *J. Appl. Comput. Mech.*, 8(1), 2022, 331–339. <https://doi.org/10.22055/JACM.2021.38487.3240>

**Publisher's Note** Shahid Chamran University of Ahvaz remains neutral with regard to jurisdictional claims in published maps and institutional affiliations.

